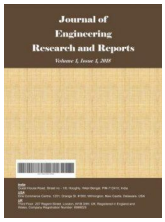

*Journal of Engineering Research and Reports*

*3(2): 1-13, 2018; Article no.JERR.45452*

# A Computerized Boundary Element Algorithm for Modeling and Optimization of Complex Magneto-Thermoelastic Problems in MFGA Structures

**Mohamed Abdelsabour Fahmy[1,2*], Saleh M. Al-Harbi[1] , Badr Hamedy Al-Harbi[1] and Alanod M. Sibih[1]**

*[1]Department of Mathematics, Jamoum University College, Umm Al-Qura University, Makkah, Saudi Arabia.*
*[2]Department of Basic Sciences, Faculty of Computers and Informatics, Suez Canal University, Ismailia, Egypt.*

***Authors' contributions***

*This work was carried out in collaboration between all authors. All authors read and approved the final manuscript.*

***Article Information***

DOI: 10.9734/JERR/2018/v3i216872
Editor(s):
(1) Dr. Anuj Kumar Goel, Associate Professor,Maharishi Markandeshwar University, (Deemed to be University), Ambala, India.
Reviewers:
(1) Francisco Bulnes, Technological Institute of High Studies of Chalco, Mexico.
(2) Jungki Lee, Hongik University, South Korea.
Complete Peer review History: http://www.sciencedomain.org/review-history/28098

***Original Research Article***

***Received 10 October 2018***
***Accepted 17 December 2018***
***Published 03 January 2019***

## ABSTRACT

**Aims:** The aim of this article is to propose a boundary integral equation algorithm for modeling and optimization of magneto-thermoelastic problems in multilayered functionally graded anisotropic (MFGA) structures.
**Study Design:** Original research paper.
**Place and Duration of Study:** Jamoum laboratory, January 2018.
**Methodology:** a new dual reciprocity boundary element algorithm was implemented for solving the governing equations of magneto-thermoelastic problems in MFGA structures.
**Results:** A numerical results demonstrate validity, accuracy, and efficiency of the presented technique.
**Conclusion:** Our results thus confirm the validity, accuracy, and efficiency of the proposed technique. It is noted that the obtained dual reciprocity boundary element method (DRBEM) results are more accurate than the FEM results, the DRBEM is more efficient and easy to use than FEM because it only needs the boundary of the domain needs to be discretized.

**Corresponding author: Email: maselim@uqu.edu.sa;*

*Keywords: Predictor-corrector; shape optimization; magneto-thermoelasticity; functionally graded anisotropic structures; dual reciprocity boundary element method.*

**2010 mathematics subject classification:** 65M38 - 65K05 - 74B05 - 74E05 - 74F05 - 74H05 - 74H15 - 74S20 - 90C31.

## 1. INTRODUCTION

An understanding of behaviour of functionally graded anisotropic magneto-thermoelastic materials has great practical applications in applied sciences and engineering. In recent years, many researchers discussed the behavior of MFGA structures. With the new advances in computer hardware and software, it is now possible to solve complex magneto-thermoelastic problems by using the DRBEM. which proposed by Nardini and Brebbia [1]. The interested readers can find more details in the following references [2-6].

The aim of this article is to propose a new DRBEM algorithm for solving the governing equations of magneto-thermoelastic problems in MFGA structures. The obtained numerical results demonstrate validity, accuracy, and efficiency of the proposed technique.

## 2. FORMULATION OF THE PROBLEM

Consider a MFGA structure occupies the region $R = \{(x, y, z): 0 < x < h, 0 < y < b, 0 < z < a\}$. At each and every point on the boundary $C$, the temperature and displacement are suitably specified.

According to Green and Naghdi theory, the governing equations of MFGA structures for the $i$th layer, can be expressed as [7-10]:

$$\sigma_{ab,b} + \tau_{ab,b} = \rho^i (x+1)^m \ddot{u}_a^i \tag{1}$$

$$\sigma_{ab} = (x+1)^m \left[ C_{abfg}^i u_{f,g}^i - \beta_{ab}^i (T^i - T_0 + \tau_1 \dot{T}^i) \right] \tag{2}$$

$$\tau_{ab} = \mu^i (x+1)^m \left( \tilde{h}_a H_b + \tilde{h}_b H_a - \delta_{ba} (\tilde{h}_f H_f) \right) \tag{3}$$

$$\left[ \left( k_{ab}^{i*} + k_{ab}^i \frac{\partial}{\partial \tau} \right) \right] T_{,ab}^i + \rho^i \dot{\mathfrak{X}} = \beta_{ab}^i T_0 \ddot{u}_{a,b}^i + \rho^i c^i (x+1)^m \ddot{T}^i \tag{4}$$

where $\sigma_{ab}$ , $\tau_{ab}$ , $u_k^i$ and $T^i$ are respectively mechanical stress, $\tau_{ab}$ Maxwell's stress, displacement and temperature, $T_0$, $C_{abfg}^i$, $\beta_{ab}^i$, $\mu^i$, $\tilde{h}$, $k_{ab}^i$ $k_{ab}^{i*}$, $\rho^i$ and $\tau$ are respectively reference temperature, constant elastic moduli, stress-temperature coefficients, magnetic permeability, perturbed magnetic field, thermal conductivity coefficients, new material coefficients associated with the GN theories, density and time, $c^i$ is the specific heat capacity, $\tau_1$ is the relaxation times, $\mathfrak{X}$ is the heat source, ; $i = 1, 2, \dots, n-1$ . represents the parameters in multilayered plate, respectively, and $f(x)$ is a given nondimensional function of space variable $x$. We take $f(x) = (x+1)^m$ , where $m$ is a dimensionless constant.

## 3. DRBEM IMPLEMENTATION

Using the same technique of Fahmy [11-13] for the current problem and implementing the DRBEM, we can write the boundary integral representation formula of coupled thermoelasticity as follows:

$$U_D^i(\xi) = \int_C \left( U_{DA}^{i*} T_A^i - \tilde{T}_{DA}^{i*} U_A^i \right) dC + \sum_{q=1}^{E} \left( U_{DE}^{iq}(\xi) + \int_C \left( T_{DA}^{i*} U_{AE}^{iq} - U_{DA}^{i*} T_{AE}^{iq} \right) dC \right) \alpha_E^q \tag{5}$$

According to Fahmy [14], the DRBEM equation (5) can be written as:

$$\check{\zeta} U - \eta T = \left( \zeta \breve{U} - \eta \breve{\wp} \right) \alpha \tag{6}$$

An implicit-implicit staggered algorithm based on DRBEM was implemented for for solving the governing equations which can be written using (6) as follows:

$$\bar{\bar{M}} \ddot{U}^i + \bar{\bar{\Gamma}} \dot{U}^i + \bar{\bar{K}} U^i = \bar{\bar{\mathbb{Q}}}^i \tag{7}$$

$$\bar{\bar{\mathbb{X}}} \ddot{T}^i + \bar{\bar{\mathbb{A}}} \dot{T}^i + \bar{\bar{\mathbb{B}}} T^i = \bar{\bar{\mathbb{Z}}} \ddot{U}^i + \bar{\bar{\mathbb{R}}} \tag{8}$$

where the matrices in (7) and (8) are as follows:

$$V = \left(\eta\breve{\wp} - \zeta\breve{U}\right)J^{-1}, \qquad \bar{\bar{M}} = V\left(\bar{\mathcal{J}} + \bar{\delta}_{AF}\right), \qquad \bar{\bar{\Gamma}} = V\bar{\Gamma}_{AF},$$
$$\bar{\bar{K}} = -\zeta' + V\left(\mathcal{B}^T J'^{-1} + \bar{\psi}\right), \qquad \bar{\bar{\mathbb{Q}}}^i = -\eta\dot{T} + V\check{S}^0, \qquad \bar{\bar{\mathsf{X}}} = -\rho^i c^i (x+1)^m,$$
$$\bar{\bar{\mathsf{A}}} = k_{ab}^i \frac{\partial}{\partial x_a}\frac{\partial}{\partial x_b}, \qquad \bar{\bar{\mathsf{B}}} = k_{ab}^{i*} \frac{\partial}{\partial x_a}\frac{\partial}{\partial x_b}, \qquad \bar{\bar{\mathbb{Z}}} = \beta_{ab}^i T_0,$$
$$\bar{\bar{\mathbb{R}}} = -\rho^i \ddot{\mathfrak{x}}.$$

Equations (7) and (8) yield the following system [15]:

$$\bar{\bar{M}}\,\ddot{U}_{n+1}^i + \bar{\bar{\Gamma}}\,\dot{U}_{n+1}^i + \bar{\bar{K}}\,U_{n+1}^i = \bar{\bar{\mathbb{Q}}}_{n+1}^{ip} \tag{9}$$

$$\bar{\bar{\mathsf{X}}}\,\ddot{T}_{n+1}^i + \bar{\bar{\mathsf{A}}}\,\dot{T}_{n+1}^i + \bar{\bar{\mathsf{B}}}\,T_{n+1}^i = \bar{\bar{\mathbb{Z}}}\,\ddot{U}_{n+1}^i + \bar{\bar{\mathbb{R}}} \tag{10}$$

where $\bar{\bar{\mathbb{Q}}}_{n+1}^{ip} = \eta T_{n+1}^{ip} + V\check{S}^0$ and $T_{n+1}^{ip}$ is the predicted temperature.

Integrating Eq. (7) and using Eq. (9), we get

$$\begin{aligned}\dot{U}_{n+1}^i &= \dot{U}_n^i + \frac{\Delta\tau}{2}\left(\ddot{U}_{n+1}^i + \ddot{U}_n^i\right)\\ &= \dot{U}_n^i + \frac{\Delta\tau}{2}\left[\ddot{U}_n^i + \bar{\bar{M}}^{-1}\left(\bar{\bar{\mathbb{Q}}}_{n+1}^{ip} - \bar{\bar{\Gamma}}\,\dot{U}_{n+1}^i - \bar{\bar{K}}\,U_{n+1}^i\right)\right]\end{aligned} \tag{11}$$

$$\begin{aligned}U_{n+1}^i &= U_n^i + \frac{\Delta\tau}{2}\left(\dot{U}_{n+1}^i + \dot{U}_n^i\right)\\ &= U_n^i + \Delta\tau\dot{U}_n^i + \frac{\Delta\tau^2}{4}\left[\ddot{U}_n^i + \bar{\bar{M}}^{-1}\left(\bar{\bar{\mathbb{Q}}}_{n+1}^{ip} - \bar{\bar{\Gamma}}\,\dot{U}_{n+1}^i - \bar{\bar{K}}\,U_{n+1}^i\right)\right]\end{aligned} \tag{12}$$

From Eq. (11) we have

$$\dot{U}_{n+1}^i = \bar{\mathsf{Y}}^{-1}\left[\dot{U}_n^i + \frac{\Delta\tau}{2}\left[\ddot{U}_n^i + \bar{\bar{M}}^{-1}\left(\bar{\bar{\mathbb{Q}}}_{n+1}^{ip} - \bar{\bar{K}}\,U_{n+1}^i\right)\right]\right] \tag{13}$$

where $\bar{\mathsf{Y}} = \left(I + \frac{\Delta\tau}{2}\bar{\bar{M}}^{-1}\bar{\bar{\Gamma}}\right)$

Substituting from Eq. (13) into Eq. (12), we derive

$$\begin{aligned}U_{n+1}^i &= U_n^i + \Delta\tau\dot{U}_n^i + \frac{\Delta\tau^2}{4}\\ &\left[\ddot{U}_n^i + \bar{\bar{M}}^{-1}\left(\bar{\bar{\mathbb{Q}}}_{n+1}^{ip} - \bar{\bar{\Gamma}}\,\bar{\mathsf{Y}}^{-1}\left[\dot{U}_n^i + \frac{\Delta\tau}{2}\left[\ddot{U}_n^i + \bar{\bar{M}}^{-1}\left(\bar{\bar{\mathbb{Q}}}_{n+1}^{ip} - \bar{\bar{K}}\,U_{n+1}^i\right)\right]\right] - \bar{\bar{K}}\,U_{n+1}^i\right)\right]\end{aligned} \tag{14}$$

Substituting $\dot{U}_{n+1}^i$ from Eq. (13) into Eq. (9) we obtain

$$\ddot{U}_{n+1}^i = \bar{\bar{M}}^{-1}\left[\bar{\bar{\mathbb{Q}}}_{n+1}^{ip} - \bar{\bar{\Gamma}}\left[\bar{\mathsf{Y}}^{-1}\left[\dot{U}_n^i + \frac{\Delta\tau}{2}\left[\ddot{U}_n^i + \bar{\bar{M}}^{-1}\left(\bar{\bar{\mathbb{Q}}}_{n+1}^{ip} - \bar{\bar{K}}\,U_{n+1}^i\right)\right]\right]\right] - \bar{\bar{K}}\,U_{n+1}^i\right] \tag{15}$$

Integrating Eq. (8) and using Eq. (10) we have

$$\begin{aligned}\dot{T}_{n+1}^i &= \dot{T}_n^i + \frac{\Delta\tau}{2}\left(\ddot{T}_{n+1}^i + \ddot{T}_n^i\right)\\ &= \dot{T}_n^i + \frac{\Delta\tau}{2}\left(\bar{\bar{\mathsf{X}}}^{-1}\left[\bar{\bar{\mathbb{Z}}}\,\ddot{U}_{n+1}^i + \bar{\bar{\mathbb{R}}} - \bar{\bar{\mathsf{A}}}\,\dot{T}_{n+1}^i - \bar{\bar{\mathsf{B}}}\,T_{n+1}^i\right] + \ddot{T}_n^i\right)\end{aligned} \tag{16}$$

$$T_{n+1}^i = T_n^i + \frac{\Delta\tau}{2}(\dot{T}_{n+1}^i + \dot{T}_n^i)$$
$$= T_n^i + \Delta\tau\dot{T}_n^i + \frac{\Delta\tau^2}{4}\left(\ddot{T}_n^i + \bar{\bar{\mathrm{X}}}^{-1}\left[\bar{\bar{\mathbb{Z}}}\,\ddot{U}_{n+1}^i + \bar{\bar{\mathbb{R}}} - \bar{\bar{\mathrm{A}}}\,\dot{T}_{n+1}^i - \bar{\bar{\mathrm{B}}}\,T_{n+1}^i\right]\right) \quad (17)$$

From Eq. (16) we get

$$\dot{T}_{n+1}^i = \mathrm{Y}^{-1}\left[\dot{T}_n^i + \frac{\Delta\tau}{2}\left(\bar{\bar{\mathrm{X}}}^{-1}\left[\bar{\bar{\mathbb{Z}}}\,\ddot{U}_{n+1}^i + \bar{\bar{\mathbb{R}}} - \bar{\bar{\mathrm{B}}}\,T_{n+1}^i\right] + \ddot{T}_n^i\right)\right] \quad (18)$$

where $\mathrm{Y} = \left(I + \frac{1}{2}\bar{\bar{\mathrm{A}}}\,\Delta\tau\,\bar{\bar{\mathrm{X}}}^{-1}\right)$

Substituting from Eq. (18) into Eq. (17), we have

$$T_{n+1}^i = T_n^i + \Delta\tau\dot{T}_n^i + \frac{\Delta\tau^2}{4}\left(\ddot{T}_n^i + \bar{\bar{\mathrm{X}}}^{-1}\left[\bar{\bar{\mathbb{Z}}}\,\ddot{U}_{n+1}^i + \bar{\bar{\mathbb{R}}}\right.\right.$$
$$\left.\left. - \bar{\bar{\mathrm{A}}}\left(\mathrm{Y}^{-1}\left[\dot{T}_n^i + \frac{\Delta\tau}{2}\left(\bar{\bar{\mathrm{X}}}^{-1}\left[\bar{\bar{\mathbb{Z}}}\,\ddot{U}_{n+1}^i + \bar{\bar{\mathbb{R}}} - \bar{\bar{\mathrm{B}}}\,T_{n+1}^i\right] + \ddot{T}_n^i\right)\right] - \bar{\bar{\mathrm{B}}}\,T_{n+1}^i\right)\right) \quad (19)$$

Substituting $\dot{T}_{n+1}^i$ from Eq. (18) into Eq. (10) we obtain

$$\ddot{T}_{n+1}^i = \bar{\bar{\mathrm{X}}}^{-1}\left[\bar{\bar{\mathbb{Z}}}\,\ddot{U}_{n+1}^i + \bar{\bar{\mathbb{R}}}\right.$$
$$\left. - \bar{\bar{\mathrm{A}}}\left(\mathrm{Y}^{-1}\left[\dot{T}_n^i + \frac{\Delta\tau}{2}\left(\bar{\bar{\mathrm{X}}}^{-1}\left[\bar{\bar{\mathbb{Z}}}\,\ddot{U}_{n+1}^i + \bar{\bar{\mathbb{R}}} - \bar{\bar{\mathrm{B}}}\,T_{n+1}^i\right] + \ddot{T}_n^i\right)\right]\right) - \bar{\bar{\mathrm{B}}}\,T_{n+1}^i\right] \quad (20)$$

Using the algorithm of Fahmy [16-22], we have the temperature and the displacements.

## 4. SHAPE DESIGN SENSITIVITY ANALYSIS AND OPTIMIZATION

Thus, the design sensitivities with respect to the design variables $x_h$ for the displacement and temperature which describe the structural response are performed by implicit differentiation of equations (9) and (10), respectively.

Let $R$ be a region with boundary C and continuous functions $m$ and $w$ satisfy

$$\iint_R \left(\frac{\partial w}{\partial x_1} - \frac{\partial m}{\partial x_2}\right) dx_1 dx_2 = \int_{\mathrm{C}} (m\,dx_1 + w\,dx_2) \quad (21)$$

The area $\bar{A} = \frac{1}{2}\int_{P_1}^{P_2} r^2 d\theta = \iint_R dx_1 dx_2$ of the domain R can be written over the boundary using the Green's theorem as [16-18]

$$\bar{A} = \frac{1}{2}\int_{\mathrm{C}} (x_1\,dx_2 - x_2\,dx_1) \quad (22)$$

By discretizing the boundary of the structure into $Q$ quadratic boundary elements, we have the following relation at $c$th element

$$x_m(\xi) = N^c(\xi)x_m^c \quad (23)$$

Also, the area can be expressed as follows

$$\bar{A} = \frac{1}{2}\sum_{b=1}^{Q}\int_{-1}^{1}[x_1(\xi)n_1 + x_2(\xi)n_2]J(\xi)d\xi \quad (24)$$

where $n_1$ and $n_2$ can be written in terms of the Jacobian matrix of the transformation $J(\xi)$ as

$$n_1 = \frac{dx_2}{d\bar{A}} = \frac{dx_2/d\xi}{d\bar{A}/d\xi} = \frac{dx_2/d\xi}{J(\xi)} \tag{25}$$

$$n_2 = -\frac{dx_1}{d\bar{A}} = -\frac{dx_1/d\xi}{d\bar{A}/d\xi} = -\frac{dx_1/d\xi}{J(\xi)} \tag{26}$$

Substitution of equations (25) and (26) into equation (24) yields

$$\bar{A} = \frac{1}{2}\sum_{b=1}^{Q}\int_{-1}^{1}\left[x_1(\xi)\frac{dx_2}{d\xi} - x_2(\xi)\frac{dx_1}{d\xi}\right]d\xi \tag{27}$$

By differentiating (27) taking into consideration that

$$\frac{\partial}{\partial x_h}\left(\frac{dx_2(\xi)}{d\xi}\right) = 0 \tag{28}$$

and

$$\frac{\partial}{\partial x_h}\big(x_2(\xi)\big) = 0 \tag{29}$$

Therefore

$$\frac{\partial \bar{A}}{\partial x_h} = \frac{1}{2}\sum_{b=1}^{Q}\int_{-1}^{1}\left[\frac{\partial x_1(\xi)}{\partial x_h}\frac{dx_2}{d\xi} - x_2(\xi)\frac{\partial}{\partial x_h}\left(\frac{dx_1}{d\xi}\right)\right]d\xi \tag{30}$$

If $x_h$ is the $x_2$ coordinate of a movable node, then

$$\frac{\partial}{\partial x_h}\left(\frac{dx_1(\xi)}{d\xi}\right) = 0 \tag{31}$$

and

$$\frac{\partial}{\partial x_h}\big(x_1(\xi)\big) = 0 \tag{32}$$

Therefore

$$\frac{\partial \bar{A}}{\partial x_h} = \frac{1}{2}\sum_{b=1}^{Q}\int_{-1}^{1}\left[x_1(\xi)\frac{\partial}{\partial x_h}\left(\frac{dx_2}{d\xi}\right) - \frac{\partial x_2(\xi)}{\partial x_h}\left(\frac{dx_1}{d\xi}\right)\right]d\xi \tag{33}$$

where weight minimization is equivalent to area minimization.

Now, we consider the following minimization problem

Minimize $\bar{A}(x_h)$ (34)

Subject to $\chi_m(x_h) \le 0, \quad \mathfrak{m} = 1, \dots, M$ (35)

$$x_h^{\omega} \le x_h \le x_h^{\varpi} \tag{36}$$

where $x_h = [x_1, x_2, \dots, x_L]^T$.

The feasible direction method (FDM) can be successfully applied for solving the current optimization problem using the following iteration process:

$$x_h = x_{h-1} + s_h d_h \tag{37}$$

Under the following condition

$$\bar{A}(x_h) - \bar{A}(x_{h-1}) \leq \varepsilon \tag{38}$$

where $h$, ε, $s_h$ and $d_h$ are respectively iteration number, predefined tolerance, line step parameter, search direction $d_h$ which can be defined as

$$d_h = -H^h \nabla \bar{A}(x_h) \tag{39}$$

where the inverse Hessian matrix can be approximated in terms of the identity matrix $I$ by

$$H^{h+1} = \left[I - \frac{P^h Q^h}{(P^h)^T Q^h}\right] H^h \left[I - \frac{Q^h (P^h)^T}{(P^h)^T Q^h}\right] + \frac{P^h (Q^h)^T}{(P^h)^T Q^h} \tag{40}$$

In which

$$P^h = x_{h+1} - x_h, \quad Q^h = \nabla \bar{A}(x_{h+1}) - \nabla \bar{A}(x_h), \quad H^0 = I$$

Using FDM, we have

$$\nabla \bar{A}(x_h) d \leq 0 \tag{41}$$

and

$$\nabla \chi_m(x_h) d \leq 0 \tag{42}$$

Now, we want to solve the following search direction problem [19]

Maximize $\mathcal{B}$

Subject to $d^T \nabla \chi_m(x_h) + \theta_m \mathcal{B} \leq 0$ (43)

$$d^T \nabla \bar{A}(x_h) + \mathcal{B} \leq 0 \tag{44}$$

$$-1 \leq d \leq 1 \tag{45}$$

where $\theta_m$ is the push-off factor which can be written as

$$\theta_m = \left[1 - \frac{\chi_m(x_h)}{\varepsilon}\right]^2 \theta_0 \tag{46}$$

where $\varepsilon$ and $\theta_0$ are constants.

We will use the preceding formulation when the design is inside the feasible domain. But when the design is outside the feasible domain, we will solve the following search direction problem

Maximize $\nabla \bar{A}(x_h).d + \Phi \mathcal{B}$

Subject to $\nabla \chi_m(x_h).d + \theta_m \mathcal{B} \leq 0, \ m \in J$ (47)

$$d^T.d \leq 1 \tag{48}$$

where $J$ and $\Phi$ are respectively potential constraint set and weighting factor.

## 5. NUMERICAL RESULTS AND DISCUSSION

In order to illustrate the numerical results of the current study, the following physical constants for material "A" are as follows

Elasticity tensor

$$C_{pjkl} = \begin{bmatrix} 430.1 & 130.4 & 18.2 & 0 & 0 & 201.3 \\ 130.4 & 116.7 & 21.0 & 0 & 0 & 70.1 \\ 18.2 & 21.0 & 73.6 & 0 & 0 & 2.4 \\ 0 & 0 & 0 & 19.8 & -8.0 & 0 \\ 0 & 0 & 0 & -8.0 & 29.1 & 0 \\ 201.3 & 70.1 & 2.4 & 0 & 0 & 147.3 \end{bmatrix} \text{GPa}$$

Mechanical temperature coefficient

$$\beta_{pj} = \begin{bmatrix} 1.01 & 2.00 & 0 \\ 2.00 & 1.48 & 0 \\ 0 & 0 & 7.52 \end{bmatrix} \cdot 10^6 \ \text{N/Km}^2$$

Tensor of thermal conductivity

$$k_{pj} = \begin{bmatrix} 5.2 & 0 & 0 \\ 0 & 7.6 & 0 \\ 0 & 0 & 38.3 \end{bmatrix} \text{W/Km}$$

Mass density $\rho = 7820$ kg/m$^3$ and heat capacity $c = 461$ J/kg K.

A prismatic material is taken as material **B** in the numerical calculations with the following physical constants

Elasticity tensor

$$C_{pjkl} = \begin{bmatrix} 60.23 & 18.67 & 18.96 & -7.69 & 15.60 & -25.28 \\ 18.67 & 21.26 & 9.36 & -3.74 & 4.21 & -8.47 \\ 18.96 & 9.36 & 47.04 & -8.82 & 15.28 & -8.31 \\ -7.69 & -3.74 & -8.82 & 10.18 & -9.54 & 5.69 \\ 15.60 & 4.21 & 15.28 & -9.54 & 21.19 & -8.54 \\ -25.28 & -8.47 & -8.31 & 5.69 & -8.54 & 20.75 \end{bmatrix} \text{GPa}$$

Mechanical temperature coefficient

$$\beta_{pj} = \begin{bmatrix} 0.002 & 0.02 & 0.03 \\ 0.02 & 0.004 & 0.04 \\ 0.03 & 0.04 & 0.05 \end{bmatrix} \cdot 10^6 \ \text{N/Km}^2$$

Tensor of thermal conductivity

$$k_{pj} = \begin{bmatrix} 0.8 & 0.1 & 0.15 \\ 0.1 & 0.9 & 0.12 \\ 0.15 & 0.12 & 0.7 \end{bmatrix} \text{W/Km}$$

Mass density $\rho = 1600$ kg/m$^3$ and heat capacity $c = 0.1$ J/kg K.
Also, a monoclinic North Sea sandstone reservoir rock is taken as material **C** in the numerical computations with the following physical constants

Elasticity tensor

$$C_{pjkl} = \begin{bmatrix} 17.77 & 3.78 & 3.76 & 0.24 & 0.28 & 0.03 \\ 3.78 & 19.45 & 4.13 & 0 & 0 & 1.13 \\ 3.76 & 4.13 & 21.79 & 0 & 0 & 0.38 \\ 0 & 0 & 0 & 8.30 & 0.66 & 0 \\ 0 & 0 & 0 & 0.66 & 7.62 & 0 \\ 0.03 & 1.13 & 0.38 & 0 & 0 & 7.77 \end{bmatrix} \text{GPa}$$

Mechanical temperature coefficient

$$\beta_{pj} = \begin{bmatrix} 0.001 & 0.02 & 0 \\ 0.02 & 0.006 & 0 \\ 0 & 0 & 0.05 \end{bmatrix} \cdot 10^6 \ \text{N/Km}^2$$

Tensor of thermal conductivity

$$k_{pj} = \begin{bmatrix} 1 & 0.1 & 0.2 \\ 0.1 & 1.1 & 0.15 \\ 0.2 & 0.15 & 0.9 \end{bmatrix} \text{W/Km}$$

Mass density $\rho = 2216$ kg/m$^3$ and heat capacity $c = 0.1$ J/kg K.

**Table. 1. Optimization analysis for considered materials**

| Material | Iterations | Percentage change between final and initial value | Maximum stress | Reduction of compliance |
|---|---|---|---|---|
| A | 12 | 65% | 0.411 | 92.40 |
| B | 12 | 65% | 0.390 | 90.87 |
| C | 12 | 73% | 0.223 | 91.10 |

**Table 2. Comparison of computer resources needed for FEM and DRBEM modelling of the right half of the link plate design**

| | FEM | DRBEM |
|---|---|---|
| Number of elements | 12980 | 48 |
| CPU-Time [min.] | 190 | 3 |
| Memory [Mbyte] | 140 | 0.6 |
| Disc space [Mbyte] | 200 | 0 |
| Accuracy of results [%] | 2.3 | 1.3 |

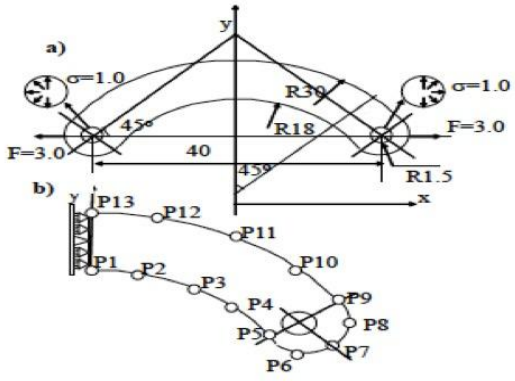


**Fig. 1. a) Geometry, b) Boundary element model for the link plate.**

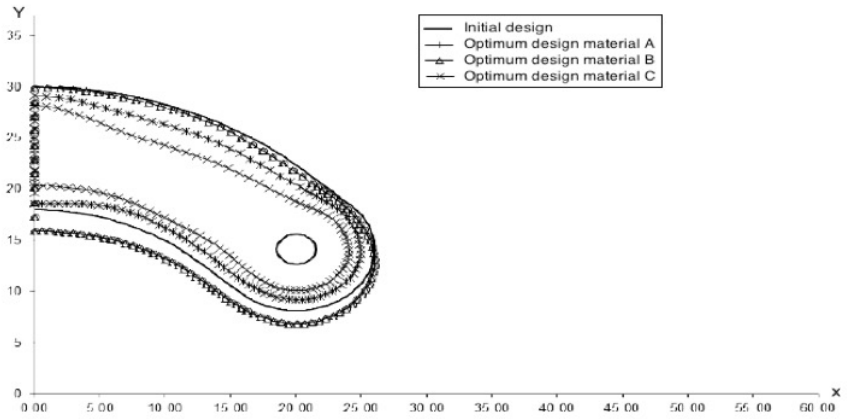


**Fig. 2. Optimum shape design for the link plate.**

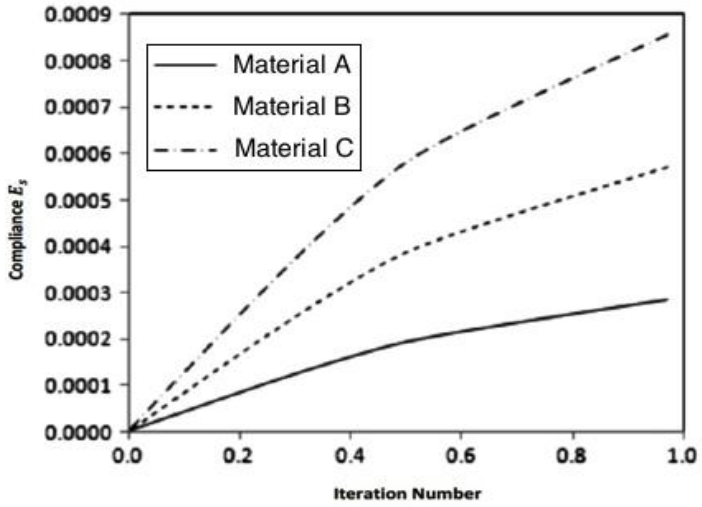


**Fig. 3. Compliance iteration history for the link plate.**

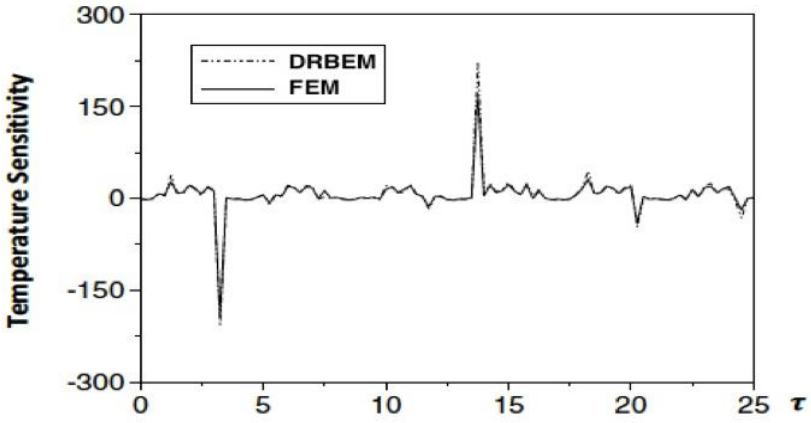


**Fig. 4. Variation of the temperature $T$ sensitivity with time $\tau$.**

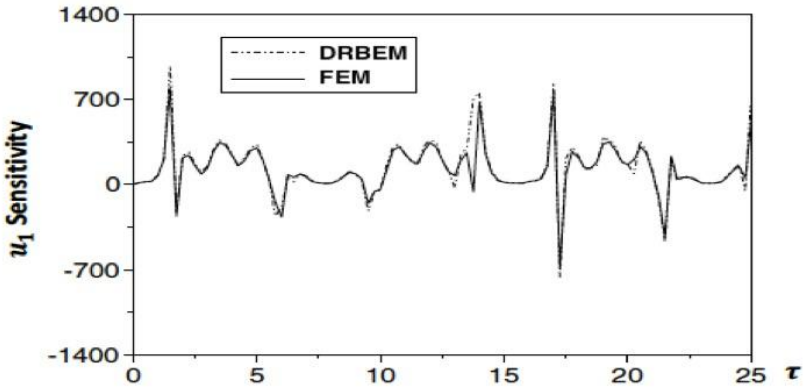


**Fig. 5. Variation of the displacement $u_1$ sensitivity with time $\tau$.**

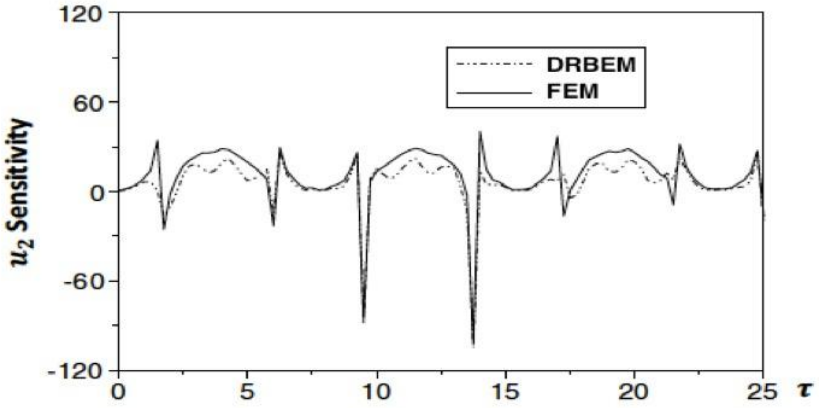


**Fig. 6. Variation of the displacement $u_2$ sensitivity with time $\tau$.**

For the purpose of numerical calculations of materials A, B and C, we considered the following constants

$H_0 = 1000000$ Oersted, $\mu = 0.5$ Gauss/Oersted, $\tau_0 = 0.5$, $m = 0.5$, $\Delta\tau = 0.0001$, $Q_0 = 0.5$, $v = 1$.

It can be noticed from numerical results that the DRBEM results are in very good agreement with those obtained using the finite element method (FEM) of Gao and Yao [23]. The right half of the link plate shown in Fig. 1a and design variables shown in Fig. 1b are considered. The optimum shapes of the considered structure for selected anisotropic materials produced from the current study are shown in Fig. 2. It can be seen that the weight and the maximum stress have increased. Fig. 3 shows the iteration history for elastic compliance of the link plate for selected materials A, B and C. It can be seen that the weight and the maximum stress of the link plate have been decreased (see Table 1). Figs. 4 and 5 show the sensitivities of the displacement distributions. Also, Fig. 6 shows the sensitivity of the temperature distribution to demonstrate the accuracy of the current technique technique (see Table 2). For further finite difference method details, we refer the reader to many researchers [24-29]. Also, for more boundary element method details we refer the reader to many researchers [30-55].

## 6. CONCLUSION

Our results thus confirm the validity, accuracy, and efficiency of the proposed technique. It is noted that the obtained dual reciprocity boundary element method (DRBEM) results are more accurate than the FEM results, the DRBEM is more efficient and easy to use than FEM because it only needs the boundary of the domain needs to be discretized.

## COMPETING INTERESTS

Authors have declared that no competing interests exist.

## REFERENCES


1. Nardini D, Brebbia CA. A new approach to free vibration analysis using boundary elements. Boundary elements in engineering, ed. Brebbia CA. Springer, Berlin; 1982.
2. Partridge PW, Brebbia CA, Wrobel LC. The dual reciprocity boundary element method. Computational Mechanics Publications, Southampton; 1992.
3. Partridge PW, Wrobel LC. The dual reciprocity boundary element method for spontaneous ignition. Int. J. Numer. Methods Eng. 1990;30:953–963.
4. Partridge PW, Brebbia CA. Computer implementation of the BEM dual reciprocity method for the solution of general field equations. Commun. Appl. Numer. Math. 1990;6:83-92.
5. Brebbia CA, Telles JCF, Wrobel L. Boundary element techniques in Engineering. Springer-Verlag, New York; 1984.
6. Gaul L, Kögl M, Wagner M. Boundary element methods for engineers and scientists, Springer-Verlag, Berlin; 2003.
7. Fahmy MA. A time-stepping DRBEM for magneto-thermo-viscoelastic interactions in a rotating nonhomogeneous anisotropic solid. International Journal of Applied Mechanics. 2011;3:1-24.
8. Fahmy MA. A time-stepping DRBEM for the transient magneto-thermo-visco-elastic stresses in a rotating non-homogeneous anisotropic solid. Engineering Analysis with Boundary Elements. 2012;36:335-345.
9. Fahmy MA. Transient magneto-thermoviscoelastic plane waves in a non-homogeneous anisotropic thick strip subjected to a moving heat source. Applied Mathematical Modelling. 2012;36:4565-4578.
10. Fahmy MA. The effect of rotation and inhomogeneity on the transient magneto-thermoviscoelastic stresses in an anisotropic solid. ASME Journal of Applied Mechanics. 2012;79:1015.
11. Fahmy MA. Transient magneto-thermo-elastic stresses in an anisotropic viscoelastic solid with and without a moving heat source. Numerical Heat Transfer, Part A: Applications. 2012;61: 633-650.
12. Fahmy MA. Implicit-explicit time integration DRBEM for generalized magneto-thermoelasticity problems of rotating anisotropic viscoelastic functionally graded solids. Engineering Analysis with Boundary Elements. 2013;37:107-115.
13. Fahmy MA. Generalized magneto-thermo-viscoelastic problems of rotating functionally graded anisotropic plates by the dual reciprocity boundary element method. Journal of Thermal Stresses. 2013;36:1-20.
14. Fahmy MA. A three-dimensional generalized magneto-thermo-viscoelastic problem of a rotating functionally graded anisotropic solids with and without energy dissipation. Numerical Heat Transfer, Part A: Applications. 2013;63:713-733.
15. Fahmy MA. A computerized DRBEM model for generalized magneto-thermo-visco-elastic stress waves in functionally graded anisotropic thin film/substrate structures. Latin American Journal of Solids and Structures. 2014;11:386-409.
16. Fahmy MA. A predictor-corrector time-stepping DRBEM for shape design sensitivity and optimization of multilayer FGA structures. Transylvanian Review. 2017;XXV:5369-5382.
17. Fahmy MA. Computerized boundary element solutions for thermoelastic problems: Applications to functionally graded anisotropic structures, LAP Lambert Academic Publishing, Saarbrücken, Germany; 2017.
18. Fahmy MA. Boundary element computation of shape sensitivity and optimization: Applications to functionally graded anisotropic structures. LAP Lambert Academic Publishing, Saarbrücken, Germany; 2017.
19. Fahmy MA. Shape design sensitivity and optimization for two-temperature generalized magneto - thermoelastic problems using time-domain DRBEM. Journal of Thermal Stresses. 2018;41:119-138.
20. Fahmy MA. Shape design sensitivity and optimization of anisotropic functionally graded smart structures using bicubic B-splines DRBEM. Engineering Analysis with Boundary Elements. 2018;87:27-35.
21. Fahmy MA. Modeling and optimization of anisotropic viscoelastic porous structures

using CQBEM and moving asymptotes algorithm. Arabian Journal for Science and Engineering; 2018.

22. Fahmy MA. Boundary element algorithm for modeling and simulation of dual phase lag bioheat transfer and biomechanics of anisotropic soft tissues. International Journal of Applied Mechanics. 2018; 10(10).
23. Gao J, Yao W. Thermal stress analysis for bi-modulus foundation beam under nonlinear temperature difference. International Journal of Computational Methods. 2017;14:1750024.
24. Akbari MR, Ghanbari J. Analytical solution of thermo-elastic stresses and deformation of functionally graded rotating hollow discs with radially varying thermo-mechanical properties under internal pressure. CMC. 2015;45(3):187-201.
25. Fahmy MA. Thermal stresses in a spherical shell under three thermoelastic models using FDM. International Journal of Numerical Methods and Applications. 2009;2:123–128.
26. El-Naggar AM, Abd-Alla AM, Fahmy MA, Ahmed SM. Thermal stresses in a rotating non-homogeneous orthotropic hollow cylinder. Heat and Mass Transfer. 2002; 39:41-46.
27. Abd-Alla AM, El-Naggar AM, Fahmy MA. Magneto-thermoelastic problem in non-homogeneous isotropic cylinder. Heat and Mass Transfer. 2003;39:625-629.
28. El-Naggar AM, Abd-Alla AM, Fahmy MA. The propagation of thermal stresses in an infinite elastic slab. Applied Mathematics and Computation. 2003;12:220-226.
29. Fahmy MA. Finite difference algorithm for transient magneto-thermo-elastic stresses in a non-homogeneous solid cylinder. International Journal of Materials Engineering and Technology. 2010;3:87-93.
30. Abd-Alla AM, El-Shahat TM, Fahmy MA. Thermal stresses in a rotating non-homogeneous anisotropic elastic multi-layered solids, Far East Journal of Applied Mathematics. 2007;27(2):223-243.
31. Abd-Alla AM, El-Shahat TM, Fahmy MA. Effect of inhomogeneity on the thermoelastic stresses in micro-engineering anisotropic solid. Far East Journal of Applied Mathematics. 2007; 27(2):245-264.
32. Abd-Alla AM, El-Shahat TM, Fahmy MA. Thermoelastic stresses in inhomogeneous anisotropic solid in the presence of body force. International Journal of Heat & Technology. 2007;25(1):111-118.
33. Abd-Alla AM, Fahmy MA, El-Shahat TM. Magneto-thermo-elastic stresses in inhomogeneous anisotropic solid in the presence of body force. Far East Journal of Applied Mathematics. 2007;27(3):499-516.
34. Abd-Alla AM, Fahmy MA, El-Shahat TM. Transient piezothermoelastic stresses in a rotating non-homogeneous composite structure. Far East Journal of Applied Mathematics. 2007;27(3):489-497.
35. Fahmy MA. Effect of initial stress and inhomogeneity on magneto-thermo-elastic stresses in a rotating anisotropic solid. JP Journal of Heat and Mass Transfer. 2007; 1:93-112.
36. Abd-Alla AM, Fahmy MA, El-Shahat TM. Magneto-thermo-elastic problem of a rotating non-homogeneous anisotropic solid cylinder. Archive of Applied Mechanics. 2008;78(2):135-148.
37. Fahmy MA. Thermoelastic stresses in a rotating non- homogeneous anisotropic body. Numerical Heat Transfer, Part A: Applications. 2008;53(9):1001-1011.
38. Fahmy MA, El-Shahat TM. The effect of initial stress and inhomogeneity on the thermoelastic stresses in a rotating anisotropic solid. Archive of Applied Mechanics. 2008;78(6):431-442.
39. Fahmy MA, Salama SA. Boundary element solution of steady-state temperature distribution in non-homogeneous media. Far East Journal of Applied Mathematics. 2010;43(1):31-40.
40. Fahmy MA. Application of DRBEM to non steady-state heat conduction in non-homogeneous anisotropic media under various boundary elements. Far East Journal of Mathematical Sciences. 2010; 43(1):83-93.
41. Fahmy MA. Influence of inhomogeneity and initial stress on the transient magneto-thermo-visco-elastic stress waves in an anisotropic solid. World Journal of Mechanics. 2011;1:256-265.
42. Fahmy MA. A time-stepping DRBEM for magneto-thermo-viscoelastic interactions in a rotating nonhomogeneous anisotropic solid. International Journal of Applied Mechanics. 2011;3:1-24.
43. Fahmy MA, Saleh Manea Al-Harbi, Badr Hamedy Al-Harbi. Implicit time-stepping DRBEM for design sensitivity analysis of

magneto-thermo- elastic FGA structure under initial stress. American Journal of Mathematical and Computational Sciences. 2017;2:55-62.

44. Fahmy MA. The effect of anisotropy on the structure optimization using golden-section search algorithm based on BEM. Journal of Advances in Mathematics and Computer Science. 2017;25:1-18.
45. Fahmy MA. DRBEM sensitivity analysis and shape optimization of rotating magneto-thermo-viscoelastic FGA structures using golden-section search algorithm based on uniform bicubic B-splines. Journal of Advances in Mathematics and Computer Science. 2017;25(6):1-20.
46. Fahmy MA. The DRBEM solution of the generalized magneto-thermo-viscoelastic problems in 3D anisotropic functionally graded solids. Idelsohn I, Papadrakakis M, Schrefler B (eds.). 5th International conference on coupled problems in science and engineering Ibiza, Spain. 2013;862-872.
47. Fahmy MA. Boundary element solution of 2D coupled problem in anisotropic piezoelectric FGM plates. Proceedings of the, Schrefler B, Oñate E, Papadrakakis M. (eds.). 6th International conference on computational methods for coupled problems in science and engineering (Coupled Problems 2015). Venice. Italy. 2015;382-391.
48. Fahmy MA. 3D DRBEM modeling for rotating initially stressed anisotropic functionally graded piezoelectric plates. 7th European congress on computational methods in applied sciences and engineering (ECCOMAS 2016). Papadrakakis M, Papadopoulos V, Stefanou G, Plevris V (eds.). Crete Island, Greece. 2016;7640-7658.
49. Fahmy MA. A time-stepping DRBEM for 3D anisotropic functionally graded piezoelectric structures under the influence of gravitational waves. Rodrigues H, Elnashai A, Calvi GM (eds.). Facing the challenges in structural engineering, sustainable civil infrastructures, proceedings of the 1st GeoMEast International Congress and Exhibition (GeoMEast 2017), Sharm El Sheikh, Egypt. 2017;350-365.
50. Fahmy MA, Salem AM, Metwally MS, Rashid MM. Computer implementation of the DRBEM for studying the generalized thermoelastic responses of functionally graded anisotropic rotating plates with one relaxation time. International Journal of Applied Science and Technology. 2013; 3(7):130-140.
51. Fahmy MA, Salem AM, Metwally MS, Rashid MM. Computer implementation of the DRBEM for studying the classical uncoupled theory of thermoelasticity of functionally graded anisotropic rotating plates. International Journal of Engineering Research and Applications. 2013;3(6): 1146-1154.
52. Fahmy MA, Salem AM, Metwally MS, Rashid MM. computer implementation of the DRBEM for studying the classical coupled thermoelastic responses of functionally graded anisotropic plates. Physical Science International Journal. 2014;4(5):674-685.
53. Fahmy MA, Salem AM, Metwally MS, Rashid MM. Computer implementation of the DRBEM for studying the generalized thermo elastic responses of functionally graded anisotropic rotating plates with two relaxation times. British Journal of Mathematics & Computer Science. 2014; 4(7):1010-1026.
54. Fahmy MA. A 2D time domain DRBEM computer model for magneto-thermoelastic coupled wave propagation problems. International Journal of Engineering and Technology Innovation. 2014;4(3):138-151.
55. Fahmy MA. Numerical modeling of coupled thermoelasticity with relaxation times in rotating FGAPs subjected to a moving heat source. Physical Science International Journal. 2016;9(4):1-13.



*Peer-review history:*
*The peer review history for this paper can be accessed here:*
*http://www.sciencedomain.org/review-history/28098*